Software for industrial scale oil production optimization

Horsholt, S.; Nick, H. M.; Jørgensen, J. B.

Important note
To cite this publication, please use the final published version (if applicable).
Please check the document version above.

P083

Software For Industrial Scale Oil Production Optimization

S. Horsholt* (Technical University of Denmark), H.M. Nick (Danish Hydrocarbon Research and Technology Centre), J.B. Jørgensen (Technical University of Denmark)

Summary

Oil production optimization of petroleum reservoirs under uncertainty give rise to large-scale optimization problems.

Ensemble-based methods for production optimization are used in combination with gradient-based optimization algorithms.

Use of commercial-grade simulators able to handle real-scale reservoir models and compute the gradient by the adjoint method is essential for implementing such methods in real-life.

However, the simulation time for a single ensemble model renders the problem computationally intractable.

Therefore, model reduction is needed.

We introduce a grid coarsening method that maintains the overall dynamics of the flow, by preserving the geological features of the model.

In this paper, we present a software tool for oil production optimization and a semi-automated workflow for grid coarsening and property upscaling.

The software tool integrates state-of-the-art optimization algorithms, ensemble-based optimization strategies and reservoir simulators with adjoint capability.

The software is based on the Eclipse input file-format, which enables use of existing reservoir models for production optimization.

This allows for oil production optimization of both black-oil and compositional flow models and brings model based production optimization a step closer to routinely implementation in reservoir management workflow.

We present the workflow of the optimization software and numerical examples that demonstrates the application of ensemble-based production optimization.

Introduction

With the modern reservoir characterization and geological modeling techniques geologists and engineers build more and more detailed reservoir models. The increasing level of available data allows geologist to build models that can account for the heterogeneity with increasing resolution. Geological reservoir models encompass detailed heterogeneous geological information at multiple length scales in different directions. Often geological models is of the size, 10^7 to 10^8 cells, which despite the computational capabilities of modern computers is too large to simulate. To build reservoir models at a scale manageable for computer simulation it is necessary to reduce the number of grid cells and upscale grid cell properties, e.g. porosity and absolute permeability. Upscaling techniques that capture the heterogeneity effects of a high-resolution model has been a long-time focus of the research community. The methods encompass simple statistical averaging techniques as well as more sophisticated numerical flow-based methods. Flow-based methods cover a range of techniques that solve a steady-state fluid flow problem over a region of the grid with no source terms. Renard and De Marsily (1997) and Barker and Thibeau (1997) provide reviews of upscaling techniques for permeability and pseudorelative permeabilities. The typical size range of upscaled reservoir models is about, 10^5 to 10^6 cells, with simulation times on the scale of hours. The industry uses these multi-phase reservoir simulation models for prediction purposes including production optimization. Frequent simulation of modern reservoir models requires a considerable computational capabilities, even by today's standards. Production optimization workflows require a potentially large number of reservoir simulations, even when applying adjoint gradient-based methods (Brouwer and Jansen, 2004; Sarma et al., 2006). In many cases, the simulation time of renders the direct use of high-fidelity models intractable. The computational burden of the optimal control problem solved in a deterministic production optimization procedure depends on the size of the simulation model, the number of control variables and control intervals. Different reduced-order modeling methods that enable approximate yet accurate simulation of complex models, has been proposed by van Doren et al. (2005) and by Cardoso and Durlofsky (2010). In order to reduce the computational effort needed in production optimization Oliveira and Reynolds (2015) propose the use of a hierarchical multiscale method for coarsening the control interval parametrization, based on control value and gradient criteria. This approach reduces the adjoint computation effort, but not the forward simulation run-time. Aliyev and Durlofsky (2015) proposes a multilevel procedure for optimizing well-placement and well-controls. The procedure utilizes a gradient-free particle-swarm optimization algorithm. Krogstad et al. (2016) use a global upscaling procedure to compute a coarse model calibrated to specific flow scenarios and applies an adjoint gradient-based optimization procedure.

In this paper, we consider reducing the computational impact of a high-fidelity model by applying a coarsening and upscaling procedure to the high-fidelity model. The coarsening and upscaling procedure is semi-automated and aims to simplify the upscaling procedure and reduce the turnover time. The coarsening method seeks to preserve geological features important for capturing the flow dynamics of the high-resolution model. The coarsening procedure partitions a fine scale grid by an index-based vector, similar to the method presented by Lie et al. (2017). To ensure flexibility in the choice of reservoir simulators we only consider logically indexed grids, i.e. corner-point grids. Hence, grid properties such as total volume is not preserved. We apply a local single-phase procedure for absolute permeability upscaling. To capture the heterogeneous effects of the high-resolution model in the near-well regions we apply the approximate coarse scale well model, proposed by Chen and Wu (2008) to upscale the well-index of well-bore completions. In this way we, reduce the forward simulation time, while replicating the behavior of the high-fidelity model to a sufficient degree for production optimization purposes. By applying this procedure, we compute a hierarchy of coarsening/upscaling levels. We introduce a hierarchical multilevel optimization procedure that optimizes an objective over the hierarchy of coarse models. The optimization procedure integrates with the adjoint gradient-based constrained optimization software tool RESOPT. RESOPT is an internally developed optimization software tool that integrates commercial reservoir simulators and state of the art optimization software (Hørsholt et al., 2018). RESOPT implements a number of optimization strategies for deterministic optimization and optimization under uncertainty, e.g. robust optimization, mean-variance optimization, and conditional value at risk optimization. RESOPT is based on the Eclipse input-file format. This allows for the use of existing reservoir models for production optimization purposes. The software integration enables optimization

of black-oil and compositional flow reservoir models.

The paper is organized as follows. We start by describing the system of equations that govern multi-phase flow in porous media, the net present value objective and states the optimal control problem. Next we describe the coarsening procedure, the grid property upscaling procedure and the well-index upscaling procedure, followed by a description of the hierarchical multigrid optimization workflow. The next part presents two numerical examples that demonstrates the optimization workflow in deterministic water-flooding scenarios. The first example is a deterministic net present value optimization of the top 8-layers of the tenth SPE comparative solution project, SPE10 model 2(Christie and Blunt, 2001). The second example is a rate-controlled optimization of the well-known Egg-model (Jansen et al., 2013). The two cases represent different types of permeability, namely a highly heterogeneous permeability field and a channeled permeability field. Finally we provide conclusions.

Reservoir simulation and optimal control problem

In this section, we state a general formulation of the system of differential algebraic equations for multi-phase flow in porous media. We present the net present value function and the optimal control problem for oil production optimization. Aziz et al. (2005) and Chen et al. (2006) provide a detailed description of the general multi-phase flow model.

System of differential algebraic equations

The system of equations that describes the subsurface flow is in most simulators discretized in space by the finite volume method and in time by the implicit Euler method. We denote the state vector as $x(t) \in \mathbb{R}^{n_x}$, the vector of algebraic variables as $y(t) \in \mathbb{R}^{n_y}$, the vector of manipulated variables as $u(t) \in \mathbb{R}^{n_u}$, and the vector of geological parameters as θ. $u(t)$ is discretized by a zero-order-hold parametrization defined by $u(t) = u_k, t_k \leq t \leq t_{k+1}, k = 0, \dots, N-1$, where $t_N = t_f$ is the final time. After spatial discretization, we write the model equations as the system of differential-algebraic equations:

$$x(t_0) = x_0, \tag{1a}$$
$$G(x(t), y(t), \theta) = 0, \qquad t \in [t_0, t_f], \tag{1b}$$
$$\dot{x}(t) = F(y(t), u(t), \theta), \quad t \in [t_0, t_f]. \tag{1c}$$

The temporal implicit Euler discretization gives the following system of non-linear equations

$$
\begin{aligned}
R_{k+1} &= R_{k+1}(x_{k+1}, y_{k+1}, x_k, u_k; \theta) \\
&= \begin{bmatrix} x_{k+1} - x_k - \Delta t_k F(y_{k+1}, u_k, \theta) \\ G(x_{k+1}, y_{k+1}, \theta) \end{bmatrix} = 0,
\end{aligned} \tag{2}
$$

for $k \in \mathcal{N} = \{0, 1, \dots, N-1\}$.

To allow for a more compact notation, we introduce the vectors, $\bar{x} = (x_1; x_2; \dots; x_N, y_1; y_2; \dots; y_N), \bar{R} = (R_0; R_1; \dots; R_{N-1})$, and $\bar{u} = (u_0; u_1; \dots; u_{N-1})$. In compact notation we write residual equations 2 as

$$\bar{R}(\bar{x}, \bar{u}, x_0; \theta) = 0. \tag{3}$$

Net present value

We define the net present value over the life time of an oil reservoir as the function, Φ, of the states, $\bar{x}$, the operating trajectory, $\bar{u}$, the initial state, x_0, and the the geological parameters, θ. In discrete time, we write the net present value as

$$\Phi(\bar{x}, \bar{u}, x_0; \theta) = \sum_{k=0}^{N-1} J_k(x_{k+1}, u_k; \theta), \tag{4}$$

where the discounted net present value, J_k, for the k'th time interval is given by

$$J_k = \frac{\Delta t_k}{(1+d)^{t_{k+1}/t_\tau}} \left[r_o q_{Os,k+1} + r_g q_{Gs,k+1} - \left(r_w q_{Ws,k+1} + r_{w,\text{inj}} q_{w,\text{inj},k+1} \right) \right].$$ (5)

Δt_k, is the length of the k'th time interval, d is the annual discount factor, t_τ is the discount time interval. r_o and r_g are the sale prices for oil and gas. r_w is the water production cost and $r_{w,\text{inj}}$ is the water injection cost. The corresponding flow rates for oil, gas, water, and water injection are denoted as, $q_{Os}, q_{Gs}, q_{Ws}, q_{w,\text{inj}}$.

Optimal control problem

The discrete-time constrained optimal control problem for production optimization is given by (Capolei et al., 2012)

$$\max_{\bar{u} \in \mathcal{U}} \quad \psi = \psi(\bar{u}; x_0, \theta),$$ (6)

where the objective function is

$$\psi(\bar{u}; x_0, \theta) = \left\{ \Phi(\bar{x}, \bar{u}, x_0; \theta) : \bar{R}(\bar{x}, \bar{u}, x_0; \theta) = 0 \right\}.$$ (7)

In this paper, we only consider linear constraints on the input. The constraints are bounds on controls, rate of movement constraints, (rom), on controls to prevent 'large' changes, and bounds on total injection rates in each time step. We write the constraints as

$$\mathcal{U} = \left\{ \bar{u} : \bar{u}_{\min} \leq \bar{u} \leq \bar{u}_{\max}, \Delta \bar{u}_{\min} \leq \Delta \bar{u} \leq \Delta \bar{u}_{\max}, b_l \leq \bar{A}\bar{u} \leq b_u \right\}.$$ (8)

Black-box simulator

The optimization workflow we present in this paper is not dependent on any specific formulation and solution method of the flow equations (1). This means we can treat the reservoir simulator as a black-box function, $\mathscr{S}(\bar{u}; x_0, \theta)$. To be eligible for gradient-based production optimization purposes, a reservoir simulator must fulfill the following requirements. Given the initial state, x_0, an operating profile, $\bar{u}$, and a geological realization vector, θ, it must at every time-step return the states, $\bar{x}$, the net present value, ψ, and the gradient of the net present value with respect to the controls, $\nabla_{\bar{u}} \psi$.

$$[\bar{x}, \psi, \nabla_{\bar{u}} \psi] = \mathscr{S}(\bar{u}; x_0, \theta).$$ (9)

Upscaling/coarsening procedure

The oil production optimization workflow, we apply in this work uses a hierarchy of upscaled models of a high-fidelity model. In this section, we outline the workflow of the coarsening and upscaling procedure for constructing such models. We describe a practical grid-coarsening method, which for our purposes preserve the geological features of the fine grid to a satisfactory degree. We apply local flow-based upscaling for the absolute permeability and simple averaging of additive properties, e.g. porosity and net to gross. To capture the effect of fine scale heterogeneity in the near well region, we upscale the well-index.

Coarsening

The oil production optimization workflow, we apply in this work uses a hierarchy of upscaled models of a high-fidelity model. In this paper, we only consider grids with logical ijk-indexing, i.e. Cartesian and corner-point grids, where each grid cell has 6-faces. The $i-$index runs first, followed by the $j-$index

and last by the $k-$index. For a grid oriented along the principal axes of a 3-dimensional coordinate system, this is the definition of "normal reading order". A grid has a number of grid cells, N_c which is the product of grid cells in each direction. Formally a grid consists of a set of ijk-indexed grid cells, $\{c_n\}_{n=1}^{N_c}, N_c = N_x N_y N_z$.

To construct a coarse grid based on a fine grid, $\{c_n\}_{n=1}^{N_{\text{fine}}}$, we group the fine grid into a number of subsets and amalgamate them into coarse grid cells, $\{c_n\}_{n=1}^{N_{\text{coarse}}}, N_{\text{coarse}} = N_{x,\text{coarse}} N_{y,\text{coarse}} N_{z,\text{coarse}}$. An amalgamated coarse grid is represented by a partitioning vector, $p \in N_{\text{fine}}$, that maps all fine grid cell into a coarse grid cell, i.e. $p_i = j$, if the fine grid cell, c_i, belongs to coarse grid cell, c_j. In principle, this allows for grouping arbitrary selections of fine grid cells into a subset. However, we only allow amalgamation of neighboring cells in the fine grid. Since all coarse grid cells are limited to have only 6-faces, the corner nodes consists of the outermost fine grid cell corner nodes. We note that this procedure does not preserve the reservoir volume, but for the purpose of optimization, this is less important. Figure 1a shows an illustration of coarsening of a fine grid. A simple way of computing the partitioning is to divide the dimensions of the fine grid by a coarsening factor in each direction, (cf_x, cf_y, cf_z). The coarse grid dimensions are then computed by

$$(N_{x,\text{coarse}}, N_{y,\text{coarse}}, N_{z,\text{coarse}}) = (\lceil N_{x,\text{fine}}/cf_x \rceil, \lceil N_{y,\text{fine}}/cf_y \rceil, \lceil N_{z,\text{fine}}/cf_z \rceil). \qquad (10)$$

This method is useful when there are no geological features, e.g. impermeable layers, horizons and faults, to take into consideration. In the gridding process for a faulted reservoir the geologist/engineer typically tries to align the grid with the faults. In this case, we take the faults into account when creating the partition by identifying the direction and the, $ijk-$index of the faults. By applying these techniques, we can construct coarse corner-point grids that preserve the geological features of a high-fidelity model to a degree that is satisfactory for our purpose.

Flow-based upscaling

After the construction of a coarse-grid, the problem of populating the grid cell with properties, e.g. net to gross, porosity and permeability remains. There exist numerous methods for upscaling these properties. These methods includes simple averaging of properties over the fine grid to more advanced methods, such as flow-based permeability upscaling. For high-level coarsening of multi-phase flow systems, upscaling the relative permeability functions is often required. For a more detailed discussion of these methods, we refer the reader to Barker and Thibeau (1997), and Renard and De Marsily (1997).
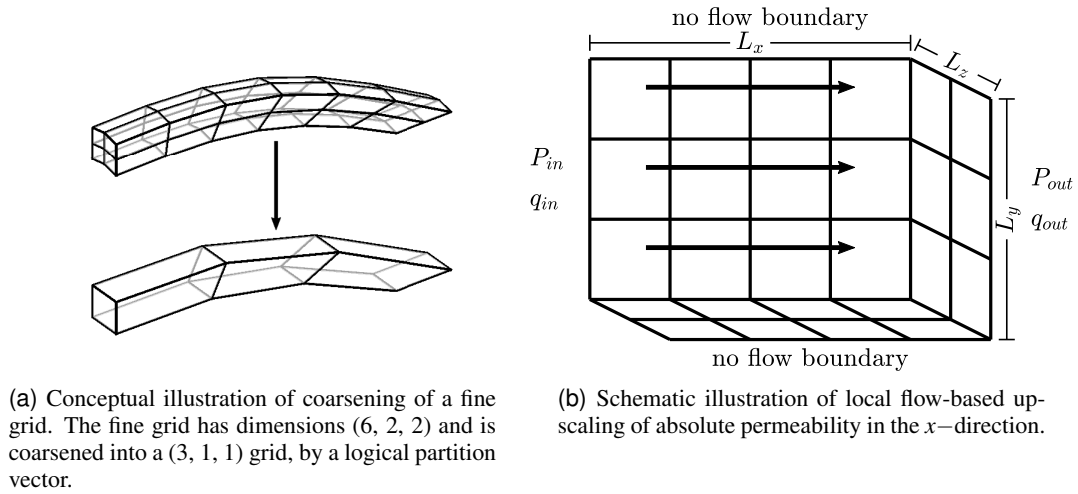
In this paper, we only consider upscaling of the grid properties, net to gross, porosity and absolute permeability. We consider arithmetic average upscaling of the porosity and net to gross properties. To upscale the absolute permeability we apply local single-phase flow-based method. By emulating a laboratory setup, we compute each component in the permeability tensor separately. The setup applies a pressure drop in each axial direction and keeps all other boundaries sealed. In the $x-$direction we compute the upscaled permeability, K_x^* in a coarse-grid cell as,

$$K_x^* = \frac{q_{x,out} L_x}{L_z L_y (P_{out} - P_{in})}, \qquad (11)$$

where, $q_{x,\text{out}}$, is the flow through the boundary, L_x, L_y, L_z, are the cell dimensions, and P_{in}, P_{out} are the pressures at the boundaries. Figure 1b shows a schematic illustration of the setup. The upscaled permeability in the, y and $z-$direction is computed in a similar fashion.

Well-index upscaling

To capture the effects of the fine scale heterogeneous permeability in the near-well regions, we upscale the well-index. We apply the 'near-well arithmetic averaging' method proposed by Chen and Wu (2008). The basis of the method is analysis of the pressure solution for two-dimensional flow in homogeneous porous media. The method applies arithmetic averaging of the effective permeabilities, K_{eff}, along the well trajectory within a coarse cell. We denote the fine scale permeability and the fine scale volume

(a) Conceptual illustration of coarsening of a fine grid. The fine grid has dimensions (6, 2, 2) and is coarsened into a (3, 1, 1) grid, by a logical partition vector.

(b) Schematic illustration of local flow-based up-scaling of absolute permeability in the $x-$direction.

Figure 1 *Conceptual illustrations of the coarsening and upscaling procedures.*
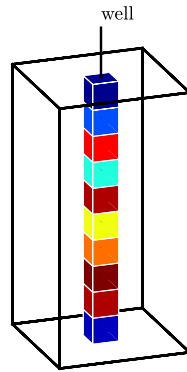
Figure 2 *Schematic illustration of near-well arithmetic averaging for a vertical well completion in a coarse cell.*

along the well trajectory in a coarse cell as, $K_{\text{fine}}, V_{\text{fine}}$, respectively. Then the near-well averaging in a given direction is calculated by

$$K_{\text{eff}} = \frac{\sum K_{\text{fine}} V_{\text{fine}}}{\sum V_{\text{fine}}}. \tag{12}$$

Figure 2 shows an illustration of the near-well arithmetic averaging for a coarse grid cell with a vertical well completion. The coarse scale well-index for a vertical well is then computed by inserting the effective permeabilities into the Peaceman model:

$$r_o = \frac{\left(\sqrt{K_{y,\text{eff}}/K_{x,\text{eff}}}\Delta x^2 + \sqrt{K_{x,\text{eff}}/K_{y,\text{eff}}}\Delta y^2\right)^{1/2}}{(K_{y,\text{eff}}/K_{x,\text{eff}})^{1/4} + (K_{x,\text{eff}}/K_{y,\text{eff}})^{1/4}}, \tag{13a}$$

$$WI_{\text{coarse}} = \frac{2\pi\sqrt{K_{x,\text{eff}}K_{y,\text{eff}}}\Delta z}{\ln(r_o/r_w)}. \tag{13b}$$

We note that this is equivalent to computing the well-index by averaging the fine scale well-index computed by the Peaceman model.

Hierarchical multigrid optimization workflow

In this section, we outline the workflow of the hierarchical multigrid optimization procedure used in this paper. In the examples presented in this paper, we select the E300 reservoir simulator from Schlumberger as the simulator and the Matlab optimization toolbox as the optimizer.
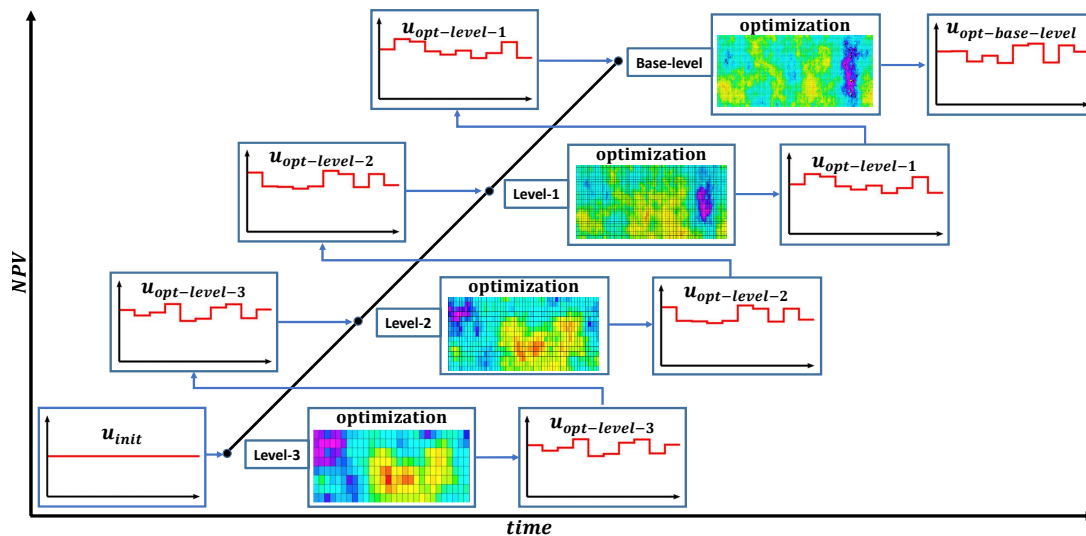
Figure 3 *Illustration of the hierarchical multigrid optimization workflow.*

Optimization workflow

The optimization workflow presented in this paper uses a hierarchy of coarse level models, based on the high-fidelity model. In the following, we refer to the high-fidelity model as the basecase and the increasing coarse model as levels, starting with the next finest level as level-1. We use the coarsening-upscaling procedure presented in the previous section to produce a hierarchy of coarse level models. The optimization procedure starts at the coarsest-level. Starting with an initial guess of the set of controls, we perform production optimization on the coarsest-level. Optimization on the subsequent levels uses the optimal set of controls computed at the previous level as start guess. At each level, we evaluate the optimal solution at the base-level. The optimization procedure can be stopped at any level depending on the aim of the optimization, time limitations and the computational resources available. Figure 3 illustrates the concept of the hierarchical multigrid optimization workflow.

Case studies

In this section, we present two case studies that demonstrate the hierarchical multigrid optimization workflow.

The first case demonstrates the workflow on the top 8-layers of the SPE10 model 2 (Christie and Blunt, 2001). The original aim of SPE10 model 2 was to compare coarsening and upscaling techniques, which makes it an ideal candidate model for testing the methods presented in this paper.

The second case is the Egg-model, which is the well-known production optimization benchmark test-case presented by Jansen et al. (2013). The Egg-model was first introduced in the robust optimization study by van Essen et al. (2009). It has been used as a benchmark test-case for optimal control method-ologies in numerous publications, e.g. by Fonseca et al. (2014), Siraj et al. (2015), Fonseca et al. (2016) and by Codas et al. (2016).

SPE10 model 2

The model reservoir model has the physical dimensions $(1200 \times 2200 \times 16)$ ft. The model is discretized into an equidistant Cartesian grid, with $(N_x, N_y, N_z) = (60, 220, 8)$ cells. The top layers is a Tarbert formation with a highly heterogeneous permeability field. The horizontal permeability ranges from 0-20000 mD with a mean of 364.5 mD and standard deviation of 1443.4 mD. The vertical permeability equals the horizontal multiplied by 0.3. The porosity has an average value of 0.175, and ranges from 0-0.5. The reservoir has a five-spot well pattern with four producers located in the reservoir corners

Table 1 *Reservoir data for the top eight-layers of the SPE10 model2.*

Description	symbol	value	metric
physical dim	(x, y, y)	$(1200, 2200, 16)$	[ft]
grid-cell dim	$(\Delta x, \Delta y, \Delta z)$	$(20, 10, 2)$	[ft]
water compressibility	c_w	1.0×10^{-6}	[psia^{-1}]
rock compressibility	c_r	1.0×10^{-6}	[psia^{-1}]
pore volume	V_{pore}	1.357×10^6	[rb]
oil in place	V_{oip}	874.93×10^3	[rb]
permeability range	(k_x, k_y)	$[0, 1200]$	[mD]
porosity range	σ	$[0, 1200]$	-
bubble-point pressure	P_b	3600	[psia]
datum pressure	P_r	3600	[psia]
datum depth	d_r	9000	[ft]
oil water contact	OWC	9100	[ft]
gas-oil contact	GOC	8800	[ft]
average water saturation	S_{wi}	0.355	-

and one water injector completed in middle of the reservoir. All wells are vertical and completed in all eight layers of the reservoir. Figure 4a shows the reservoir model. In contrast to the original model we here consider flow of a black-oil type fluid, namely the black-oil fluid from the SPE09 model (Killough, 1995). Table 1 shows the reservoir data.

Optimization parameters

We have performed a deterministic net present value optimization of the SPE10 model. Reservoir production is simulated for 3000 days in a water-flooding scenario. The simulation time interval is divided into 100 control time-steps, N, of equal length, $\Delta t = 30$days. The bottom-hole pressures in all wells are subject to control. This gives a total of 500 controls, $\bar{u}$. The bottom-hole pressure in the injection well are bounded to the interval $[3800, 5500]$ psia and the producers are bounded in the interval $[1700, 3500]$ psia. The bottom-hole pressures are constrained by a rate of movement of 30 psia between control intervals. There is no imposed constraints on the well rates and the net present value is not discounted. The optimization procedure utilizes an active-set algorithm and is initialized with a water injection pressure of 4000 psia and producer pressure of 2000 psia. Table 2 shows the optimization parameters.

Model hierarchy

We have constructed three coarsening/upscaling levels of the SPE10 model. For the coarsening procedure we apply three levels of coarsening factors, (cf_x, cf_y, cf_z), namely $(2, 2, 2), (4, 4, 4)$ and $(8, 8, 8)$. Table 3 shows the details of the coarsening procedure. The basecase properties are upscaled as decribed in section . The porosity is upscaled by arithmetic averaging. The absolute permeability is upscaled by the local flow-based method. The well-index is not upscaled, but is computed by the reservoir simulator using the standard Peaceman model. Figure 4b shows the SPE10 model hierarchy with the upscaled horizontal permeability.

Optimization procedure

We demonstrate the hierarchical multigrid optimization procedure on four constructed levels of the SPE10 model. As described previously, the hierarchical optimization starts with optimization on level-3. The computed set of optimal controls, $\bar{u}^*_{\text{opt,level-3}}$, is passed on to level-2 as initial controls, $\bar{u}_{\text{init}}$, where a new optimal set of controls, $\bar{u}_{\text{opt,level-2}}$ is computed. This procedure continues all the way to the base-case level. After applying this procedure we end up with four sets of optimal controls,

Table 2 *Optimization parameters for the deterministic net present value optimization of the top 8 layers of SPE10 model 2.*

Description	symbol	value	metric
strategy	Deterministic	-	-
simulation time	t_f	3000	[day]
number of control steps	N	100	-
length of control steps	Δt	30	[day]
number of controlled wells	n_w	5	-
number of controls	n_u	500	-
initial controls	u_{init}	-	[psia]
injector	$u_{\text{inj,init}}$	4000	[psia]
producers	$u_{\text{prod,init}}$	2000	[psia]
lower bound on controls	u_{min}	-	[psia]
injector	$u_{\text{inj,min}}$	3800	[psia]
producers	$u_{\text{prod,min}}$	5500	[psia]
upper bound on controls	u_{max}	-	[psia]
injector	$u_{\text{inj,max}}$	1700	[psia]
producers	$u_{\text{prod,max}}$	3500	[psia]
rom constraint	$\Delta\bar{u}_{\text{min}}, \Delta\bar{u}_{\text{max}}$	30	[psia]
discount factor	d	0.0	-
fluid prices:	r_α	-	[US\$/SVOL]
oil	r_o	45.00	[US\$/STB]
gas	r_g	0.0001	[US\$/SCF]
water	r_w	10.00	[US\$/STB]
water injection	$r_{w,inj}$	2.00	[US\$/STB]
algorithm	active-set	-	-
max iterations	maxit	50	-
max function evaluations	maxit	150	-
tolerance on optimimality	tol_{opt}	10^{-6}	-
tolerance on step size	$\text{tol}_{\Delta u}$	10^{-6}	[psia]
tolerance on objective	$\text{tol}_{\Delta u}$	10^3	[US\$]

Table 3 *SPE10 model grid coarsening levels*

level	coarsening factor	grid dimensions	number of cells
base-case	-	$(60, 220, 8)$	105600
level-1	$(2, 2, 2)$	$(30, 11, 4)$	13200
level-2	$(4, 4, 4)$	$(15, 55, 2)$	1650
level-3	$(8, 8, 8)$	$(8, 28, 1)$	512

$\bar{u}^*_{\text{opt,level-3}}, \bar{u}_{\text{opt,level-2}}, \bar{u}_{\text{opt,level-1}}, \bar{u}_{\text{opt,base-level}}$. Furthermore we optimize all levels individually with initial controls, $\bar{u}_{\text{init}}$, given in table 2, to obtain three additional sets of optimal controls. We refer to these by the superscript *, hence the optimal controls are denoted, $\bar{u}^*_{\text{opt,level-2}}, \bar{u}^*_{\text{opt,level-2}}, \bar{u}^*_{\text{opt,base-level}}$.

In-order to validate the results we evaluate all optimal sets of controls by simulation in the Schlumberger E100 reservoir simulator. This gives us the E100-net present value for all levels. To assess the effectiveness of the strategies, we simulate a reactive-strategy case in E100 and compute the net present value. The reactive-strategy case is simulated using the initial controls, $\bar{u}_{\text{init}}$, where a production well is shut if it becomes uneconomical, i.e. if the watercut rises above 0.88. Table 4 show the results from the hierarchical multigrid optimization and the optimization with the initial controls, $\bar{u}_{\text{init}}$, of all levels individually. Figures 5a and 5b show iteration versus net present value, including the evaluation in E100, for the hierarchical optimization procedure and the individual optimizations respectively. The results for the hierarchical optimization approach show that the net present value evaluated at the high fidelity model (E100) increases at every level in the hierarchy, as expected. There are clear jumps in the net present value when moving from one level to the next. This is expected since the coarsening/upscaling procedure does not preserve volumes, e.g. oil in place. However, this is not too important as long as the coarse levels capture the dynamics of the flow at the base-level to a reasonable degree. Figure 7 shows the optimal controls for each well at all coarsening levels. The figure clearly shows that the optimal controls computed at the coarsest level propagates through to the base-level while approximately maintaining the same shape. This suggest that the flow dynamic are preserved to a high degree at all
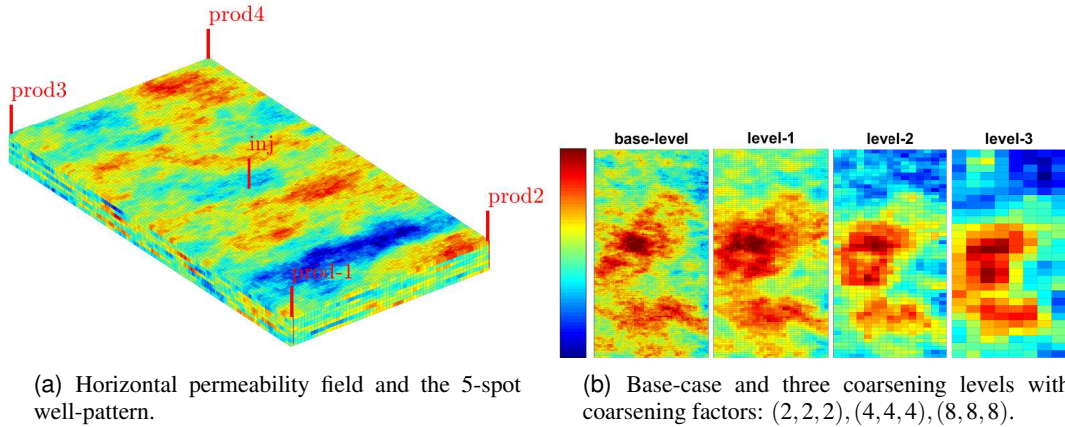
(a) Horizontal permeability field and the 5-spot well-pattern.

(b) Base-case and three coarsening levels with coarsening factors: $(2,2,2),(4,4,4),(8,8,8)$.

Figure 4 *Top 8 layers of the SPE10 model 2.*

Table 4 *SPE10 hierarchical multigrid optimization results.*

Level	# iterations	# simulations	elapsed time [hour]	flag	NPV [MMUS$]	E100
level-3*	37	76	0.2338	$\Delta\bar{u}$	9.56	8.15
level-2	14	27	0.1196	$\Delta\bar{u}$	9.41	8.24
level-1	7	17	0.3941	$\Delta\bar{u}$	8.85	8.35
base-level	3	17	13.0770	$\Delta\bar{u}$	8.38	8.43
level-2*	49	98	0.4443	$\Delta\bar{u}$	9.40	8.32
level-1*	29	57	1.6590	$\Delta\bar{u}$	8.87	8.41
base-level*	13	53	44.7560	$\Delta\bar{u}$	8.06	8.16
reactive-strategy						7.81

coarsening levels. However, there is no guarantee that the hierarchical approach will provide a higher net present value at all levels than the corresponding initial controls optimization at the same level.

Figure 6 shows the elapsed time versus net present value for all performed optimizations. The figure shows that the hierarchical approach provides the best result at the base-level (shortest computation time and highest NPV). At all levels, the hierarchical optimization converges using fewer iterations and thus computation time. However the initial control optimization of both level-2* and level-1* obtains a higher net present value than the hierarchical optimizations at the same levels. This underlines that the optimization is sensitive to the choice of initial controls. In all cases, optimization leads to a significantly higher net present value than the reactive strategy case.
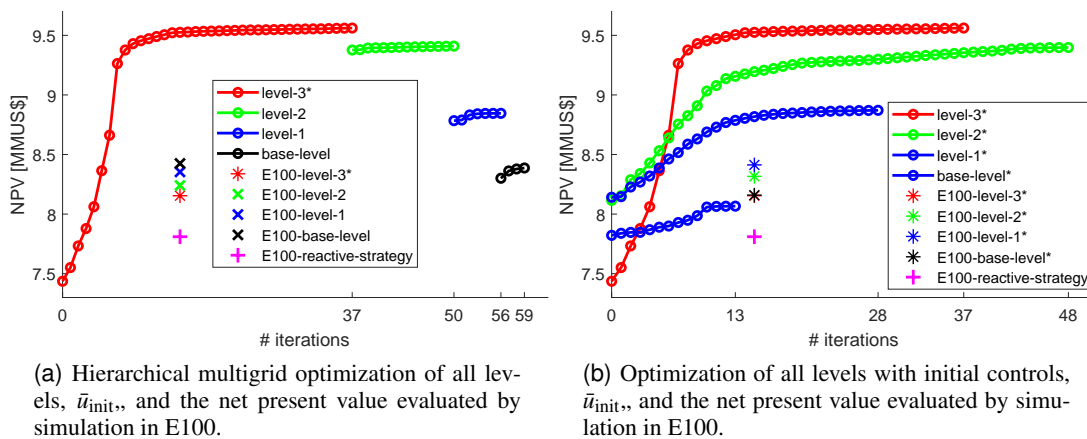

(a) Hierarchical multigrid optimization of all levels, $\bar{u}_{\text{init}}$, and the net present value evaluated by simulation in E100.

(b) Optimization of all levels with initial controls, $\bar{u}_{\text{init}}$, and the net present value evaluated by simulation in E100.

Figure 5 *Optimization of the SPE10 model 2. All points denoted E100 are placed arbitrary on the iteration axis.*
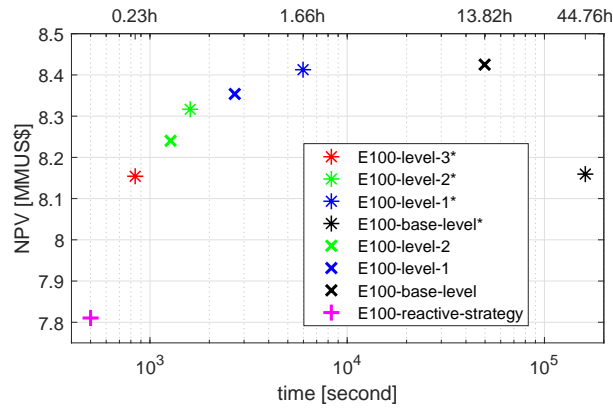
Figure 6 *Optimization of the SPE10 model, computation time versus net present value evaluated in E100.*
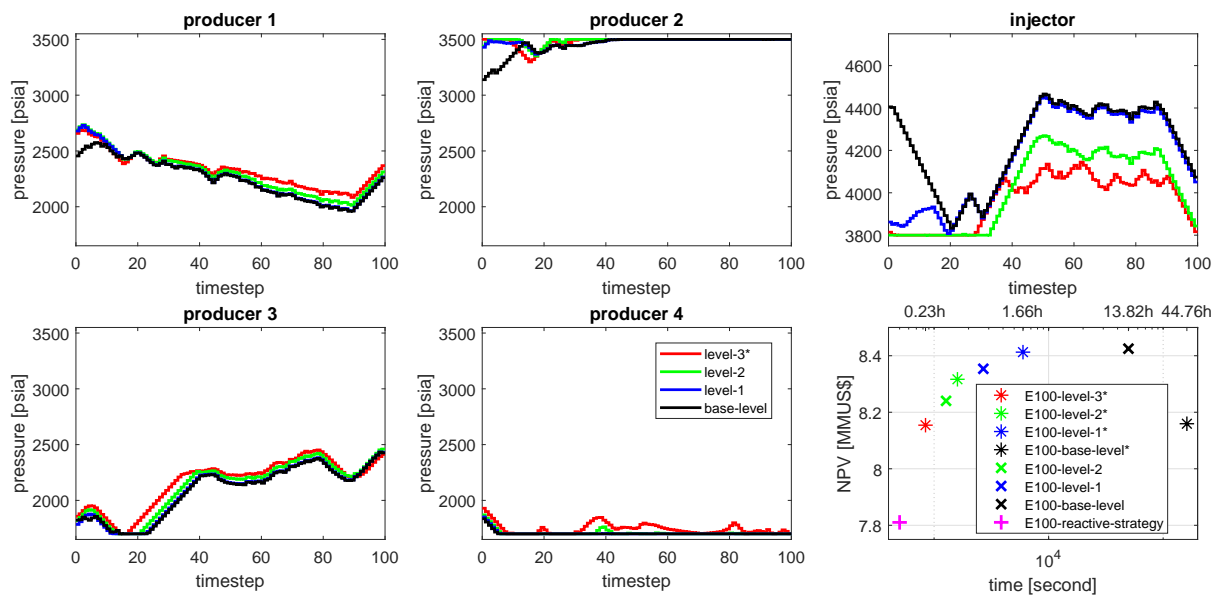

Figure 7 *Optimization of the SPE10 model. Optimal controls for all levels and computation time versus net present value evaluated in E100.*

Egg-model

The Egg-model is a three-dimensional synthetic two-phase flow reservoir model. The model consist of 101 realizations of the permeability field. In this paper, we consider only the first of these fields.

The physical reservoir dimensions is, $(480, 480, 28)$m. It is discretized on a Cartesian grid with $(N_x, N_y, N_z) = (60, 60, 7)$ cells. All grid cells have the size, $(\Delta x, \Delta y, \Delta z) = (8, 8, 4)$ m. The grid has a total of 25.200 cells where 18553 are active. The reservoir has uniform pososity, $\phi = 0.2$, and a highly channelized permeability field. The model has a total of 12 vertical wells of which eight are water injectors and four are producers. All well-bores are vertical and are completed throughout all seven layers in the $z-$direction. Figure 8a shows the permeability field for the realization used in the optimization and the well locations. The reservoir is simulated with the original two-phase fluid. Table 5 shows the reservoir model parameters. Jansen et al. (2013) provides a full description of the model.

Table 5 *Egg-model; standard reservoir and fluid data.*

description	symbol	value	Metric
grid-cell height	Δz	4	[m]
grid-cell length/width	$\Delta x, \Delta y$	8	[m]
porosity, uniform	ϕ	0.2	-
oil compressibility	c_o	10^{-5}	[1/bar]
water compressibility	c_w	10^{-5}	[1/bar]
rock compressibility	c_r	0	[1/bar]
viscosity oil	μ_o	5	[cp]
viscosity water	μ_w	1	[cp]
rel. perm end point, oil	k_{ro}^0	0.8	-
rel. perm end point, water	k_{ro}^w	0.2	-
Corey exponent, oil	n_o	4.0	-
Corey exponent, water	n_w	3.0	-
residual oil saturation	S_{or}	0.1	-
connate-water saturation	S_{wc}	0.2	-
capillary pressure	P_c	0	[bar]
initial reservoir pressure	P_{ri}	400	[bar]
initial water saturation	S_{wi}	0.	-
bhp producer wells	P_{bh}	395	[bar]
well-bore radius	r_w	0.1	[m]

Optimization parameters

The deterministic optimization is performed on the first realization of the permeability field (see Figure 8a). Reservoir production is simulated for 3600 days with 120 control time-steps of length, $\Delta t = 30$ days. The water injection rate in all injector wells are subject to control. This gives a total of 960 controls, $\bar{u}$. The bottom-hole pressures in the producers are kept constant at 395 bar throughout the simulation. All injection rates are bounded in the interval [0, 80] m³/day and are not allowed to change with a rate greater than, 5 m³/day between control steps. The discount rate, d in (5) is set to 10%. The optimization is initialized with a water injection rate of, 79.0 m³/day. The convergence tolerances for the KKT-optimality conditions, tol$_{opt}$ and the step-size, tol$_x$ are both set to 10^{-6}.

The optimization is performed by first applying a SQP-algorithm for a limited number of iterations and then switching to an interior-point algorithm until convergence. The number of SQP-iterations depends on the coarsening-level. The SQP-algorithm is more aggressive and tends to achieve good results in relatively few iterations. However it uses many line-search simulations especially when close to convergence. The interior-point algorithm on the other hand tends to apply relatively small changes to the controls, but uses fewer line-search simulations. Hence, by combining the algorithms we attempt to minimize the number of optimization iterations.

Model hierarchy

As in the previous example, we have constructed three coarsening/upscaling levels of the Egg-model.

For the coarsening procedure we apply three levels of coarsening factors, $(2, 2, 1), (4, 4, 1)$, and $(8, 8, 1)$. Thus keeping the resolution in the vertical direction constant. To determine whether a coarse cell is active or not, we consider the fine cells that it contains. If half or more of the fine cells contained in the coarse cell are active the coarse cell is set to be active and otherwise the coarse cell is set to be in-active. We note that this does not preserve the grid volume, but as mentioned earlier this is not an issue for the purpose of the optimization procedure. Table 7 shows the details of the coarsening procedure. The base-case properties are upscaled as described in section . The porosity is uniform and hence no upscaling is required. The absolute permeability is upscaled by the local flow-based method. In this example, the well-index is upscaled and written directly to the simulator. Figure 8b shows the Egg-model hierarchy with the upscaled horizontal permeability.

Table 6 *Egg-model; optimization parameters.*

Description	symbol	value	Metric
optimization strategy	deterministic	-	-
number of control steps	N	120	-
length of control steps	Δt	30	[day]
controls, water injection rates	q_{wi}	-	[m^3/day]
bound constraints	$q_{wi,\min}$	0.2	[m^3/day]
	$q_{wi,\max}$	80.0	[m^3/day]
rate of movement constraints	rom	± 5	[m^3/day]
initial controls	u_{init}	79.0	[m^3/day]
prices	r_α	-	[US\$/m^3]
	r_o	283.04	[US\$/m^3]
	r_w	37.74	[US\$/m^3]
	r_{wi}	12.58	[US\$/m^3]
discount factor	d	10%	-
optimization algorithm	SQP, interior-point	-	-
optimality tolerance	tol_{opt}	1e-6	-
step-size tolerance	tol_x	1e-6	-

Table 7: Egg-model grid coarsening levels.

Level	coarsening factor	grid dimensions	# cells	active cells
base-case	-	$(60, 60, 7)$	25200	18553
level-1	$(2, 2, 1)$	$(30, 30, 7)$	6300	4736
level-2	$(4, 4, 1)$	$(15, 15, 7)$	1575	1198
level-3	$(8, 8, 1)$	$(8, 8, 7)$	448	344

Optimization procedure

The hierarchical optimization procedure starts at level-3, where the optimization is initiated with, $\bar{u}_{\text{init}}$, stated in Table 6. The optimal controls, $\bar{u}^*_{\text{opt,level-3}}$, is passed on to the next level where it is used as the initial guess. This continues to the base-level. Hence we get four sets of optimal controls denoted, $\bar{u}^*_{\text{opt,level-3}}, \bar{u}_{\text{opt,level-2}}, \bar{u}_{\text{opt,level-1}}, \bar{u}_{\text{opt,base-level}}$. Again we optimize all levels using the initial controls, $\bar{u}_{\text{init}}$, to get the optimal controls, $\bar{u}^*_{\text{opt,level-2}}, \bar{u}^*_{\text{opt,level-1}}, \bar{u}^*_{\text{opt,base-level}}$. All sets of optimal controls are evaluated by simulation at the base-level in the E100 simulator and is compared to a reactive-strategy simulation.

As described previously we apply a combination of the SQP and the interior-point optimization algorithms. The limit of iterations and simulations depends on coarsening level and adapts to the tolerances in Table 8. For validation purposes, we evaluate the obtained optimal control sets, by simulation in the Schlumberger E100 reservoir simulator. Furthermore, we run a reactive-strategy case, also simulated in E100. The reactive-strategy case is simulated using the initial controls, $\bar{u}_{\text{init}}$, where a production well is shut if it becomes uneconomical, i.e. the water-cut rises above 0.88. Table 9 shows the results from all levels for both the hierarchical multigrid optimization procedure and for the optimization with initial
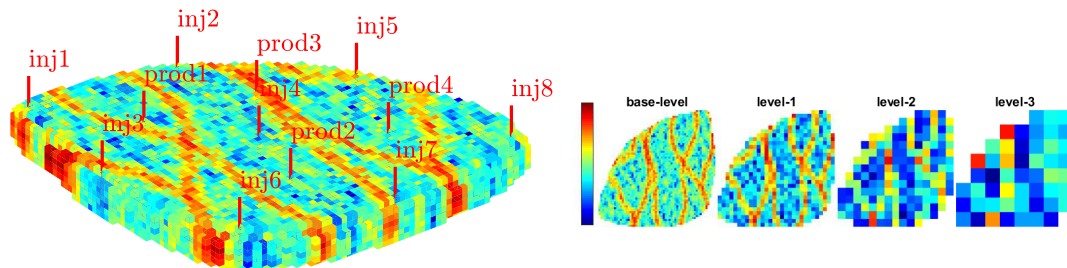
(a) Well locations and permeability field of first realization.

(b) Base-case and three coarsening levels, with coarsening factors: $(2, 2, 1), (4, 4, 1), (8, 8, 1)$.

Figure 8 *Egg-model hierarchy and well-pattern.*

Table 8 Egg-model combined SQP and interior-point strategy tolerances.

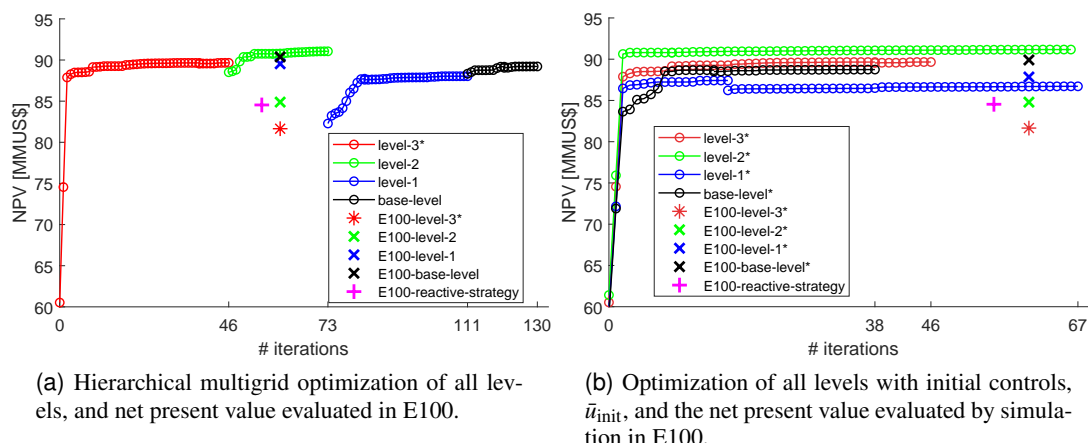|	SQP		interior-point	
level	max it	max sim	max it	max sim
level-3*	50	300	100	300
level-2	25	300	100	300
level-1	10	300	50	300
base-level	10	300	25	300
level-2*	50	300	100	300
level-1*	50	300	50	300
base-level	50	300	50	300

Table 9 Egg-model hierarchical multigrid optimization results.

level	# iterations	# simulations	elapsed time [hour]	flag	NPV [MMUS$]	E100
level-3*	46	351	2.079	max sim	89.7	81.6
level-2	27	261	1.313	$\Delta \bar{u}$	90.8	85.2
level-1	38	138	1.131	max it	87.8	88.9
base-level	19	193	8.592	max it	89.2	90.4
level-2*	66	318	1.644	$\Delta \bar{u}$	90.8	85.0
level-1*	67	370	3.532	max sim	87.4	88.4
base-level*	38	248	11.527	$\Delta \bar{u}$	88.7	89.8

controls, $\bar{u}_{\text{init}}$. Figures 9a and 9b shows iteration versus net present value, including the evaluation in E100, for the hierarchical optimization procedure and the individual optimizations respectively. As in the SPE10 example, we see clear jumps in the objective value when moving from one level to the next. This is partially an effect of the fact that the coarsening/upscaling procedure do not preserve volumes. In addition, the coarser a level is, the capture of the flow dynamic of the high-fidelity model becomes worse. However, this is expected and not significant as long as we experience an increasing objective value, when evaluated at the high-fidelity level.

Evaluation of the optimal controls computed during the hierarchical multigrid optimization procedure, shows that the net present value increases at every level. The same trend is showing in the optimizations using, $\bar{u}_{\text{init}}$, as initial controls. Optimization at the coarsest level, level-3*, is not able to provide a net present value higher than that obtained by the reactive-strategy case.

Figure 10 shows the injector rate controls computed at all levels by the hierarchical multigrid optimization procedure. There is some similarities of the controls throughout the levels, but it is not as significant as for the SPE10 case. These similarities increases for the finer levels. This suggest that the difference in the flow dynamic between the layers decreases for finer grid resolution as expected. Figure 11 shows

(a) Hierarchical multigrid optimization of all levels, and net present value evaluated in E100.

(b) Optimization of all levels with initial controls, $\bar{u}_{\text{init}}$, and the net present value evaluated by simulation in E100.

Figure 9 Optimization of the Egg-model. The points denoted E100 are placed at an arbitrary position on the iteration axis.
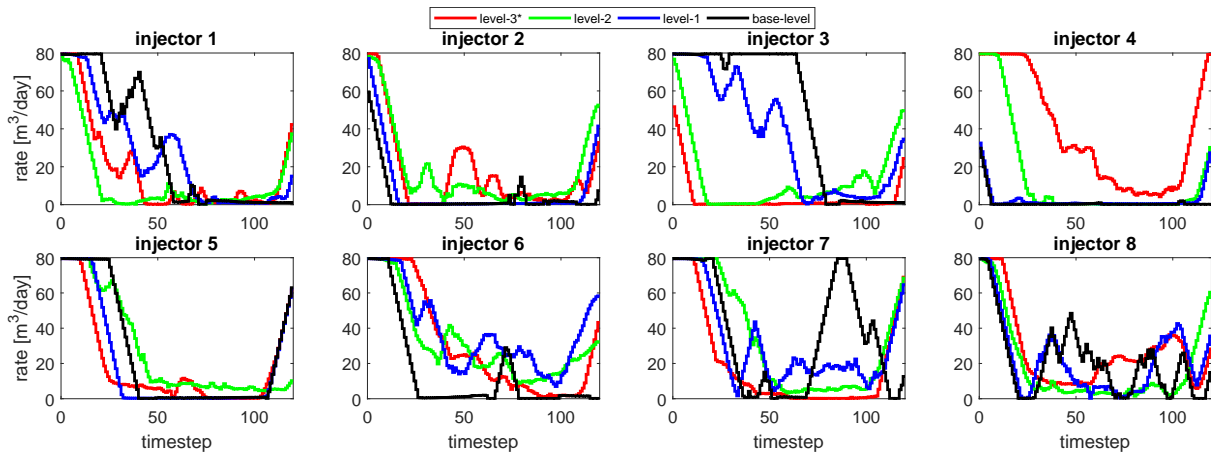
Figure 10 *Hierarchical multigrid optimization Egg-model. Optimal controls for all levels.*
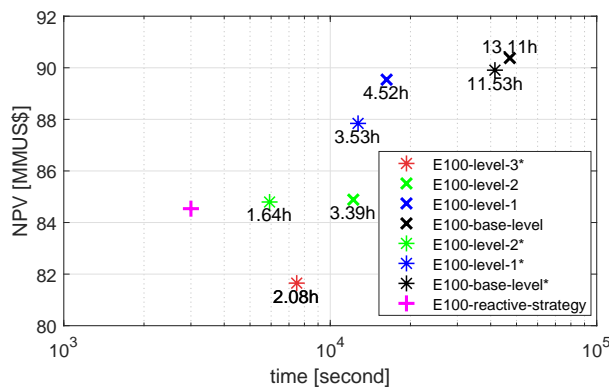

Figure 11 *Optimization of the Egg-model, computation time versus net present value evaluated in E100.*

elapsed time versus net present value for all level optimizations. At all levels we see that the hierarchical approach provides a higher net present value than the optimization using the initial controls, $\bar{u}_{\text{init}}$, at the corresponding level. The shape of the elapsed time versus net present value curve is close to the ideal as depicted in the conceptual illustration in Figure 3. We partially credit this to the relatively simple two-phase, oil-water fluid model, for which the single-phase flow-based upscaling method is better suited.

Conclusion

We have developed a hierarchical multigrid optimization procedure for oil production optimization. The base of the procedure is the Eclipse file-format, which enables the use of existing reservoir models. The procedure uses a partitioning of a high-fidelity grid to compute a number of increasing coarse level grids with upscaled properties. A gradient-based optimization software tool, (RESOPT) perform optimization on the hierarchy of models. The optimization procedure starts on the coarsest level and uses the optimal solution as the start guess on the next level. We demonstrate the optimization workflow on the SPE10 model 2. The developed procedure significantly reduces the both the simulation run time and the number of performed optimization iterations. By applying this workflow, we bring implementing optimization of industry scale reservoirs for use in reservoir management decisions a step closer.

Acknowledgements

References

Aliyev, E. and Durlofsky, L.J. [2015] Multilevel Field-Development Optimization using a Sequence of Upscaled Models. In: *SPE Reservoir Simulation Symposium*. Society of Petroleum Engineers.

Aziz, K., Durlofsky, L.J. and Tchelepi, H. [2005] Notes for petroleum reservoir simulation. *Stanford University, Stanford, Califormia, USA*.

Barker, J.W. and Thibeau, S. [1997] A Critical Review of the Use of Pseudorelative Permeabilities for Upscaling. *SPE Reservoir Engineering*, **12**(2), 138–143.

Brouwer, D.R. and Jansen, J.D. [2004] Dynamic Optimization of Waterflooding With Smart Wells Using Optimal Control Theory. *SPE Journal*, **9**(04), 391–402.

Capolei, A., Völcker, C., Frydendall, J. and Jørgensen, J.B. [2012] Oil Reservoir Production Optimization using Single Shooting and ESDIRK Methods. *IFAC Proceedings Volumes*, **45**(8), 286–291.

Cardoso, M.A. and Durlofsky, L.J. [2010] Linearized reduced-order models for subsurface flow simulation. *Journal of Computational Physics*, **229**(3), 681–700.

Chen, Y. and Wu, X.H. [2008] Upscaled modeling of well singularity for simulating flow in heterogeneous formations. *Computational Geosciences*, **12**(1), 29–45.

Chen, Z., Huan, G. and Ma, Y. [2006] *Computational methods for multiphase flows in porous media*. SIAM.

Christie, M.A. and Blunt, M.J. [2001] Tenth SPE Comparative Solution Project: A Comparison of Upscaling Techniques. In: *SPE Reservoir Simulation Symposium*. Society of Petroleum Engineers.

Codas, A., Hanssen, K.G., Foss, B., Capolei, A. and Jørgensen, J.B. [2016] Multiple Shooting applied to robust reservoir control optimization including output constraints on coherent risk measures. *Computational Geosciences*, 1–19.

van Doren, J.F.M., Markovinović, R. and Jansen, J.D. [2005] Reduced-order optimal control of water flooding using proper orthogonal decomposition. *Computational Geosciences*, **10**(1), 137–158.

van Essen, G., Zandvliet, M., Van den Hof, P., Bosgra, O. and Jansen, J.D. [2009] Robust Waterflooding Optimization of Multiple Geological Scenarios. *SPE Journal*, **14**(01), 202–210.

Fonseca, R.M., Reynolds, A.C. and Jansen, J.D. [2016] Generation of a Pareto front for a bi-objective water flooding optimization problem using approximate ensemble gradients. *Journal of Petroleum Science and Engineering*, **147**, 249–260.

Fonseca, R.M., Stordal, A.S., Leeuwenburgh, O., Van den Hof, P.M.J. and Jansen, J.D. [2014] Robust ensemble-based multi-objective optimization. In: *ECMOR XIV-14th European conference on the mathematics of oil recovery*.

Hørsholt, S., Nick, H.M. and Jørgensen, J.B. [2018] Oil Production Optimization of Black-Oil Models by Integration of Matlab and Eclipse E300. In: *3rd IFAC Workshop on Automatic Control in Offshore Oil and Gas Production*.

Jansen, J.D., Fonseca, R.M., Kahrobaei, S., Siraj, M., Van Essen, G. and Van den Hof, P. [2013] The Egg model. *Delft University of Technology, The Netherlands, Tech. Rep., Research note and data set. htt p://repository. tudelft. nl/view/ir/uuid: 1b85ee17-3e58-4fa4-be79-8328945a4491 and http://data. 3tu. nl/reposi tory/uuid: 916c86cd-3558-4672-829a-105c62985ab2(accessed 23 March 2015)*.

Killough, J.E. [1995] Ninth SPE Comparative Solution Project: A Reexamination of Black-Oil Simulation. In: *SPE Reservoir Simulation Symposium*. Society of Petroleum Engineers.

Krogstad, S., Raynaud, X. and Nilsen, H.M. [2016] Reservoir management optimization using well-specific upscaling and control switching. *Computational Geosciences*, **20**(3), 695–706.

Lie, K.A., Kedia, K., Skaflestad, B., Wang, X., Yang, Y., Wu, X.H. and Hoda, N. [2017] A General Non-Uniform Coarsening and Upscaling Framework for Reduced-Order Modeling. In: *SPE Reservoir Simulation Conference*. Society of Petroleum Engineers.

Oliveira, D.F. and Reynolds, A. [2015] Hiererarchical Multiscale Methods for Life-Cycle-Production Optimization: A Field Case Study. *SPE Reservoir Simulation Symposium*, (SPE-173273-MS).

Renard, P. and De Marsily, G. [1997] Calculating equivalent permeability: a review. *Advances in water resources*, **20**(5-6), 253–278.

Sarma, P., Durlofsky, L.J., Aziz, K. and Chen, W.H. [2006] Efficient Real-time Reservoir Management Using Adjoint-based Optimal Control and Model Updating. *Computational Geosciences*, **10**(1), 3–36.

Siraj, M.M., Van den Hof, P.M. and Jansen, J.D. [2015] Handling risk of uncertainty in model-based production optimization: a robust hierarchical approach. *IFAC-PapersOnLine*, **48**(6), 248–253.